

# Temperature and density dependence of the structural relaxation time in water by inelastic ultraviolet scattering

F. Bencivenga,<sup>a)</sup> A. Cimatoribus, A. Gessini, M. G. Izzo, and C. Masciovecchio  
*Sincrotrone Trieste, S.S. 14 km 163.5, Area Science Park, I-34012 Basovizza, Trieste, Italy*

(Received 12 June 2009; accepted 14 September 2009; published online 8 October 2009)

The density and temperature dependence of the structural relaxation time ( $\tau$ ) in water was determined by inelastic ultraviolet scattering spectroscopy in the thermodynamic range ( $P = 1\text{--}4000$  bars,  $T = 253\text{--}323$  K), where several water anomalies take place. We observed an activation (Arrhenius) temperature dependence of  $\tau$  at constant density and a monotonic density decrease at constant temperature. The latter trend was accounted for by introducing a density-dependent activation entropy associated to water local structure. The combined temperature and density behavior of  $\tau$  indicates that differently from previous results, in the probed thermodynamic range, the relaxation process is ruled by a density-dependent activation Helmholtz free energy rather than a simple activation energy. Finally, the extrapolation of the observed phenomenology at lower temperature suggests a substantial agreement with the liquid-liquid phase transition hypothesis. © 2009 American Institute of Physics. [doi:10.1063/1.3243314]

## I. INTRODUCTION

Water undoubtedly plays a central role in everyday life, and it has been intensively studied throughout the whole history of science. Although in recent times its physical behavior has been deeply investigated, its puzzling phenomenology still struggles modern scientist. In particular, the origin of water anomalies, which mostly shows up at low temperature, is currently the subject of a lively and interdisciplinary debate.<sup>1-3</sup>

Among the various attempts to elaborate a commonly accepted and comprehensive framework, the most promising ones are the liquid-liquid phase transition hypothesis<sup>4</sup> and the singularity-free scenario.<sup>5</sup> In the former case authors proposed that liquid water can exist in two distinct phases, a low-density liquid (LDL) and high-density liquid (HDL), separated by a first-order liquid-liquid phase transition. These liquid phases are associated with the two experimentally observed glassy phases of water, the low-density amorphous (LDA) and high-density amorphous (HDA) ice, which seem to be separated by a first-order transition, even if this point is still debated.<sup>3,6,7</sup> Since the LDL-HDL critical point should be located at  $T_C \approx 220$  K and  $P_C \approx 1$  kbar, “normal” liquid water is the “supercritical phase” of LDL and HDL. Water anomalies are then related to a genuine critical-like behavior, enhanced in the supercooled phase because of the proximity of the LDL-HDL critical point. Recently a very high-density amorphous (VHDA) phase was also reported.<sup>7,8</sup> The VHDA and HDA structures are quite similar and it is likely that HDA is a metastable form of VHDA.<sup>9</sup> In this case the scenario depicted above fully holds considering VHDA as the (stable) glassy phase of HDL. However, since the postulated thermodynamic singularity should be located below the homogeneous nucleation temperature ( $T_H$ ), experi-

ments on bulk liquid water close and below  $T_C$  cannot be performed. As a consequence, a direct experimental corroboration of this frame was not yet obtained. However, neutron and x-ray diffraction experiments showed a continuous change in water local structure with density and temperature above  $T_H$ . Moreover, the asymptotic low- and high-density/temperature structures are found to be similar to the LDA and HDA ones, respectively.<sup>10,11</sup> On one hand these results are consistent with a reminiscence of a LDL-HDL phase transition taking place at lower temperature but, on the other hand, they do not necessarily imply this scenario.<sup>7,12</sup> Furthermore, experimental investigations of the dynamics in the temperature ( $T$ ) and density ( $\rho$ ) range characteristic of this phenomenology are still missing. Indeed, these studies are of the greatest relevance since, according to the singularity-free scenario, water anomalies are related to the structural relaxation, typical of glass-forming systems.<sup>13</sup> In particular, the relaxation dynamics coupled with the tetrahedral water structure leads to an enhancement of cross correlations between entropy and volume fluctuations, which give rise to a behavior similar to the one observed near a critical point even in the absence of a real thermodynamic singularity.<sup>5,13,14</sup> Studies of the  $T$  dependence of the structural relaxation time ( $\tau$ ) pointed out a noteworthy low- $T$  increase in  $\tau$  (Refs. 15–17) with respect to the high- $T$  trend.<sup>18-21</sup> The observed behavior agrees with the predictions of the mode coupling theory (MCT),<sup>13</sup> a theory belonging to the class of singularity-free models. Accordingly, it was inferred that there is no need to introduce a real thermodynamic singularity for explaining water anomalies.<sup>15,16</sup> However, these experiments were performed in a  $\rho$  range limited to  $\approx 1000$  kg m<sup>-3</sup>, and neither the  $\rho$ - nor the  $T$ -dependence of  $\tau$  was determined in the ( $\rho, T$ )-region where, according to diffraction data, water undergoes the aforementioned continuous structural change. Measurements of  $\tau(\rho)$  at fixed  $T$  were recently performed by the Brillouin inelastic ultraviolet scattering (IUVS) and an

<sup>a)</sup>Electronic mail: filippo.bencivenga@elettra.trieste.it.

anomalous  $\rho$ -dependence of  $\tau$  has been observed.<sup>17,22</sup> This trend cannot be easily cast in a standard theory of structural relaxation process, such as MCT, thus challenging the interpretation of water anomalies in the singularity-free framework. However, the available data are not enough for drawing any conclusion since they fail to concurrently determine both  $T$ - and  $\rho$ -dependences.

The main aim of the present work is to fully characterize  $\tau(\rho, T)$  in the low temperature thermodynamic region of water. Here most of water anomalies, including the continuous  $(\rho, T)$ -change in water structure, takes place. For this purpose we employed IUVS spectroscopy at the BL10.2 beamline at the Elettra laboratory (Trieste, Italy).<sup>23</sup> This technique can provide a trustfully determination of  $\tau$ , while the high throughput of the employed instrument allowed mapping the rather large thermodynamic range of interest. The accuracy of the results we will show in the following indicates how IUVS can be successfully employed to study relaxation dynamics in liquids, and how this technique may present noteworthy advantages with respect to both inelastic light and x-ray scattering.

## II. EXPERIMENTAL METHODS

Brillouin spectra of bidistilled and de-ionized water were collected by the BL10.2 IUVS spectrometer<sup>23</sup> in a  $(\rho, T)$ -range extending from  $\approx 1000$  to  $\approx 1150$  kg m<sup>-3</sup> and from 323 K down to the melting temperature ( $T_M$ ).

A high purity water sample was placed in a homemade high pressure hydrostatic cell with optically polished sapphire windows. The pressure was generated by a manually driven piston connected to the high pressure cell through a capillary. The maximum pressure achievable by this setup is  $\approx 4000$  bars. The pressure cell was kept in thermal contact with a cryostat cold finger and a resistive heater. The sample temperature was electronically controlled with an  $\approx 0.2$  K accuracy, while the  $P$  stability was always better than 1%. A monochromatic UV beam with wavevector  $\lambda_i$  impinges into the sample crossing the sapphire windows. The scattered beam was collected in an almost backscattering geometry (scattering angle,  $\theta_S \approx 172^\circ$ ) and energy analyzed by an 8 m long Czerny–Turner monochromator. A position-sensitive detector was used to collect the frequency ( $\omega$ ) dependence of the scattered beam in the  $\pm 1$  THz range around  $\omega_i = 2\pi c/\lambda_i$ , with  $c$  being the speed of light. This setup allows avoiding time consuming frequency scans of scattered radiation and, therefore, greatly increases the throughput of the instrument. The overall frequency resolution was set to  $\approx 10$  GHz, while the time needed to acquire a single IUVS spectra was  $\sim 30$  min. Further details on the beamline can be found elsewhere.<sup>17,23</sup>

The  $\omega$ -dependence of IUVS signal [ $I(Q, \omega)$ , where  $Q$  is the momentum transfer] is proportional to the frequency spectrum of the density-density correlation function, i.e., the dynamical structure factor ( $S(Q, \omega)$ ),<sup>16,17,24,25</sup> plus an elastic scattering contribution (modeled by a  $\delta$ -function) convoluted with the experimental resolution function ( $R(\omega)$ ),

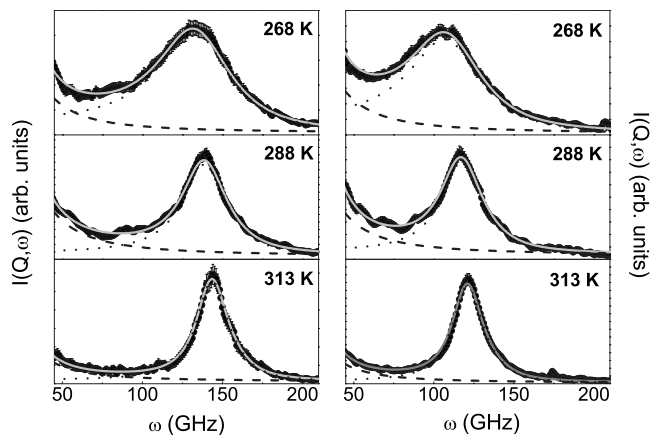


FIG. 1. Selected IUVS spectra of water at  $\rho \approx 1110$  kg m<sup>-3</sup> (left panels) and  $\rho \approx 1030$  kg m<sup>-3</sup> (right panels) at the indicated temperatures. The solid gray lines are best fit results. The dashed and dotted lines account for elastic and inelastic scatterings, respectively.

$$I(Q, \omega) \propto [A_1 S(Q, \omega) + A_2 \delta(\omega)] \otimes R(\omega) + B, \quad (1)$$

where  $\otimes$  is the convolution operator,  $B$  is a constant background,  $A_1$  and  $A_2$  are the scaling factors, while  $\delta(t)$  is the Dirac function accounting for the elastic scattering.

Figure 1 displays a selection of IUVS spectra of water together with the respective best fit results. The peak observed at  $\omega \sim 100$ – $150$  GHz is the longitudinal acoustic (LA) mode of water. Such an inelastic signal arising from LA modes was modeled by a damped harmonic oscillator (DHO) spectrum,

$$S(Q, \omega) = \frac{1}{\pi} \frac{\Omega_L^2 \Gamma_L}{[\omega^2 - \Omega_L^2]^2 + [\omega \Gamma_L]^2}, \quad (2)$$

where  $\Omega_L$  and  $\Gamma_L$  are the characteristic frequency and damping of LA modes, respectively. The former is defined as the frequency corresponding to the maxima of longitudinal current spectrum,  $J_L(Q, \omega) = (\omega/Q)^2 S(Q, \omega)$ , i.e.,

$$\left. \frac{\partial J_L(Q, \omega)}{\partial \omega} \right|_{\omega = \pm \Omega_L} = 0. \quad (3)$$

Employing some straightforward algebra it is possible to demonstrate that the DHO function fulfills the above relation. The parameters  $\Omega_L$  and  $\Gamma_L$  are also related to the longitudinal sound velocity ( $c_L$ ) and kinematic viscosity ( $\nu_L$ ) through the relations:  $\Omega_L = c_L Q$  and  $\Gamma_L = \nu_L Q^2$ , where  $Q(\rho, T, \lambda_i) = 4\pi n(\rho, T, \lambda_i) \sin(\theta_S/2)/\lambda_i$ , with  $n(\rho, T, \lambda_i)$  being the known refraction index of water.<sup>26</sup> Using Eqs. (1) and (2) for fitting IUVS spectra we obtained an accurate ( $< 1\%$ ) determination of  $\Omega_L$ .

## III. THEORETICAL BASIS

We used the memory function approach for deriving the  $(\rho, T)$ -dependence of  $\tau$  from the IUVS spectra. This formalism allowed us to exploit the well known relations between the relaxation processes of density fluctuations and the viscoelastic behavior of water.

Indeed, one of the quantities directly measurable by IUVS (i.e.,  $c_L$ ) is strongly affected by viscoelastic effects

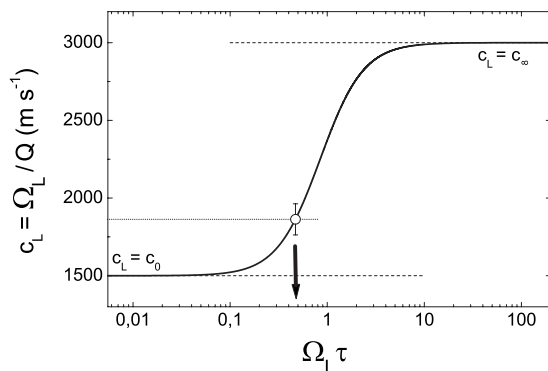


FIG. 2. Positive sound dispersion phenomenology. The full line represents the  $\Omega_L \tau$ -dependence of  $c_L$ . Horizontal dashed lines are  $c_0$  (lower line) and  $c_\infty$  (upper line). Since both of these quantities do not depend on  $\Omega_L \tau$ , they are constant parameters at a given  $(\rho, T)$ -value. The circle is an example of  $\Omega_L$  measurement from which one can derive the corresponding value of  $\tau$ , once  $c_0$ ,  $c_\infty$ , and  $Q$  are known.

associated with the occurrence of relaxation processes. Specifically,  $c_L$  undergoes a transition on increasing  $\Omega_L \tau$  between two limiting, frequency-independent, sound velocities.<sup>17–22,24,25,27–40</sup> The low frequency limit ( $c_0$ ) is reached when  $\Omega_L \tau \ll 1$  and it can be identified with the adiabatic sound velocity, which is the propagation velocity of LA modes predicted by classical hydrodynamics for a viscous fluid. The high frequency limit of  $c_L$  (hereafter reported as  $c_\infty$ ) is met for  $\Omega_L \tau \gg 1$ , and it is similar to the propagation velocity of LA modes in the amorphous solid phase, which in the case of water, is roughly twice than  $c_0$ .<sup>27–29</sup> Such a viscoelastic variation of  $c_L$  is also usually referred to as “positive sound dispersion.”

In the case of water such a positive sound dispersion phenomenology can be described in the memory function framework by assuming an exponential time decay of the memory function ( $m(Q, t)$ ):<sup>18–22,29–32</sup>

$$m(Q, t) = (c_\infty^2 - c_0^2) Q^2 \exp\{-c_\infty^2 t / c_0^2 \tau\}. \quad (4)$$

The resulting expression for  $S(Q, \omega)$  can be written as<sup>18–21,25,29,32,37–39</sup>

$$\frac{S(Q, \omega)}{S(Q)} = \frac{1}{\pi} \frac{(c_0 Q)^2 m'(Q, \omega)}{[\omega^2 - (c_0 Q)^2 - \omega m''(Q, \omega)]^2 + \omega^2 [m'(Q, \omega)]^2}, \quad (5)$$

where  $S(Q)$  is the static structure factor, while  $m'(Q, \omega)$  and  $m''(Q, \omega)$  are the real and imaginary parts of the Fourier transform of  $m(Q, t)$ , respectively. Within the assumptions summarized in Eqs. (4) and (5), and exploiting the definition of  $\Omega_L$  reported in Eq. (3), it is possible to derive an analytical relation linking  $\tau$ ,  $\Omega_L$ ,  $c_0$ ,  $c_\infty$ , and  $Q$ ,<sup>22</sup>

$$\tau = (c_\infty / c_0)^2 \sqrt{\frac{1 - (c_0 Q / \Omega_L)^4}{2c_\infty^2 Q^2 - 2\Omega_L^2}}. \quad (6)$$

The rationale of this method is sketched in Fig. 2, where the  $\Omega_L \tau$ -dependence of  $c_L = \Omega_L / Q$  is displayed. At a given  $(\rho, T)$ -value (i.e., at a given value of  $c_0$  and  $c_\infty$ ) such a de-

pendence is fully set by the hypothesis made for the time decay of  $m(Q, t)$  [i.e., by Eq. (4)]. In this case, if the  $c_L$  datum is different from  $c_0$  or  $c_\infty$ , then there is a unique value of  $\tau$  corresponding to the measured value of  $\Omega_L$ . Therefore, once  $c_0(\rho, T)$ ,  $c_\infty(\rho, T)$ , and  $Q(\rho, T)$  are independently known,  $\tau(\rho, T)$  can be derived from the  $(\rho, T)$ -dispersion of  $\Omega_L$  without employing a more sophisticated viscoelastic line shape analysis, which is usually affected by strong correlations among fitting parameters. These correlations often lead to a poor accuracy in the determination of  $\tau$ .

In the case of water  $c_0(\rho, T)$  can be calculated by the equation of state<sup>41</sup> and  $c_\infty(\rho, T)$  estimated from previous inelastic x-ray scattering (IXS) experiments.<sup>18–20,32,36,42</sup> IXS probes  $\Omega_L$ -values largely above the terahertz, the condition  $\Omega_L \tau \gg 1$  (elastic regime) is then essentially met in all the thermodynamic region explored in the present experiment. Therefore, regardless of the specific data analysis strategy, IXS provides an almost direct measure of  $c_\infty$ . In summary, using Eq. (6) we can obtain the  $(\rho, T)$ -dependence of  $\tau$  from the one of  $\Omega_L$  that, ultimately, has been straightforwardly extracted from IUVS spectra using Eqs. (1) and (2). The accuracy in the values of  $c_0(\rho, T)$  calculated by the equation of state is quite high ( $\approx 0.1\% - 0.5\%$ ),<sup>41</sup> comparable or even better than the one associated to the experimental determination of  $c_L(\rho, T)$ . Conversely, the  $c_\infty(\rho, T)$ -values have a rather poor accuracy (in some cases larger than 5%) and, furthermore, the  $(\rho, T)$ -dependence of  $c_\infty$  was derived by interpolating IXS results collected in the thermodynamic region of interests.<sup>18–20,32,36,42</sup> However, this uncertainty in the  $c_\infty$  determination only marginally affects the determination of  $\tau$  in the present case. In fact, as far as we are dealing with relatively small deviations of  $\Omega_L$  with respect to  $c_0 Q$ , the leading contribution to the experimental uncertainty ( $\delta\tau$ ) arises from the parameters  $\Omega_L$  and  $c_0$ , rather than  $c_\infty$ . Indeed, by differentiating Eq. (6) one can readily observe that  $(\partial\tau / \partial c_0) \propto [c_L^4 - c_0^4]^{-1}$ ,  $(\partial\tau / \partial \Omega_L) \propto [(c_L^4 - c_0^4)(c_\infty^2 - c_L^2)]^{-1}$ , while  $(\partial\tau / \partial c_\infty) \propto [c_\infty^2 - c_L^2]^{-1}$ . Such a relatively weak dependence of  $\tau$  from  $c_\infty$  for  $c_L \approx c_0$  also explains why previous IUVS results on water obtained with the present method are weakly sensitive to the value of  $c_\infty$  (see, e.g., Fig. 3 of Ref. 22).

Finally, it is worth stressing how, on a general ground, the optimal condition for determining  $\tau$  is met when  $\Omega_L \tau \sim (c_\infty / c_0)^2$ . In the present case this means  $\Omega_L \lesssim$  THz. Since the use of UV radiation allows measuring  $\Omega_L$ -values roughly twice larger than the ones detectable with visible light, this optimal condition is better approached.

Finally, it is worth stressing that the memory function approach does not allow to *a priori* associate a well defined dynamical process to the relaxation since  $\tau$  is a global measure of the time scale for the decay of density-density correlation function. Therefore,  $\tau$  could be, in principle, related to different molecular degrees of freedom (intermolecular bond making and breaking, collisions, rotations, vibrations, etc.), with possible different weights depending on  $\rho$  and  $T$ . However, previous investigations pointed out that in several system (water among them), the time decay of  $m(Q, t)$  observed in the probed time scale (approximately equal to picosecond) is dominated by the rearrangements of the local structure that, in the liquid phase, mainly consist in the breaking and

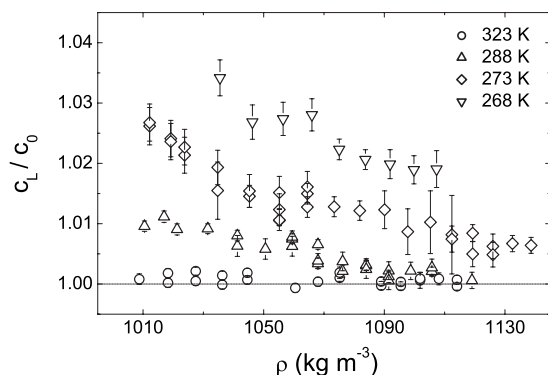


FIG. 3. Representative  $(\rho, T)$ -values of  $c_L/c_0$ . Data at 273 K are from Refs. 17 and 22.

forming of intermolecular bonds.<sup>18–21,31,32,37–40</sup> It was also widely demonstrated that  $\tau$ , as derived by the viscoelastic behavior of LA modes, can be meaningfully associated to macroscopic thermodynamic quantities.<sup>18–20,33–35,37–39</sup> On the other hand, intramolecular degrees of freedom likely result into faster relaxation processes, also referred to as instantaneous relaxations, which certainly play a role in very high frequency inelastic scattering experiments [as IXS (Refs. 19–21, 32, and 37–39)] but have negligible effects in the visible and UV range.<sup>16,17,22,31,40</sup> In summary the employed method permits to directly extract from IUVS spectra the average relaxation time decay of density fluctuations, i.e.,  $\tau$ , in the picosecond time scale, which, in water, is dominated by the dynamics of the local hydrogen bond (HB) network.

#### IV. EXPERIMENTAL RESULTS

In Fig. 3 we show some representative  $(\rho, T)$ -values of  $c_L$ , as extracted by IUVS spectra, divided by the respective values of  $c_0(\rho, T)$ .<sup>41</sup> The  $(\rho, T)$ -deviation of the former with respect to the latter is the aforementioned viscoelastic effect we are looking for in order to determine  $\tau$ . Since the larger is the value of  $\tau$ , the larger is the deviation of  $c_L$  with respect to  $c_0$ , one can readily appreciate how  $\tau$  increases both on decreasing temperature and on increasing density. These trends are more evident by looking at Figs. 4 and 5, where the

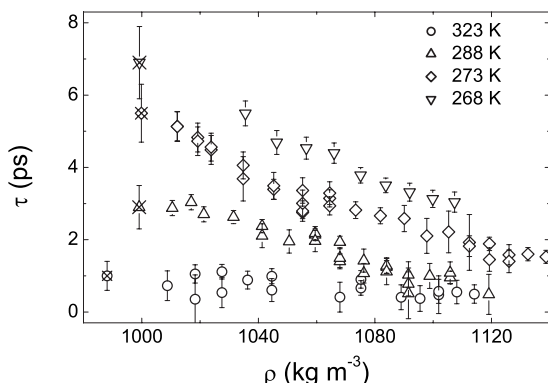


FIG. 4.  $\rho$ -dependence of  $\tau$  for some representative temperatures, as obtained from the analysis of the LA mode dispersion. Data at 273 K are from Refs. 17 and 22. Crossed symbols are room pressure data from Ref. 16, as obtained by a viscoelastic line shape analysis.

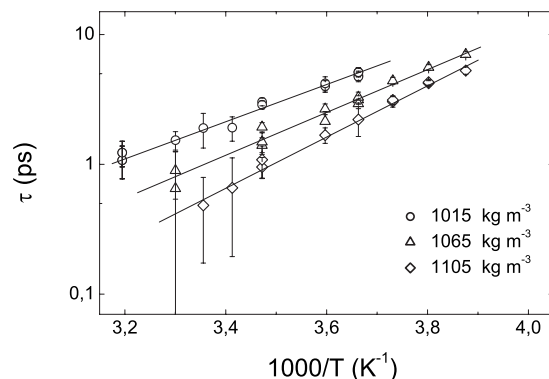


FIG. 5.  $T$ -dependence of  $\tau$  for some representative densities. The full lines highlight the activation trend [see Eq. (7)]. The different slopes of these lines indicate a change in activation energy with density.

values of  $\tau$  are reported as obtained by the method described in Sec. III.

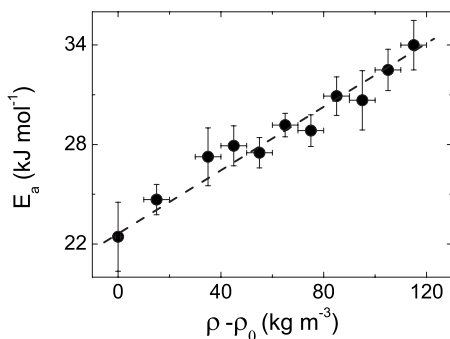
Figure 4 depicts the  $\rho$ -dependence of  $\tau$  for some representative temperatures; crossed symbols are room pressure data obtained by employing a viscoelastic data analysis.<sup>16</sup> The consistency between the two methods is evident. The decrease in  $\tau$  with increasing density is an uncommon behavior in liquids since a  $\rho$ -increase in  $\tau$  is instead expected. In fact, at high density the free volume reduction results in a slowing down of the structural relaxation time scale and a consequent reduction in molecular mobility.<sup>43</sup> At densities close to the ones of the solid phase, such a slowing down may eventually turn into a diverge and leads to a pressure induced solidification. The data reported in Fig. 4 then suggest that there are other effects that over-rule the free volume reduction and increase the mobility of the system. Indeed, an anomalous enhancement of water fluidity at high density was already observed through viscosity measurements.<sup>44</sup>

Figure 5 shows the temperature dependence of  $\tau$  for some representative densities. The data are reported in an Arrhenius plot in order to stress the activation trend, i.e.,

$$\tau \propto \exp\{E_a/k_B T\}, \quad (7)$$

where  $E_a$  and  $k_B$  are the activation energy of the structural relaxation and the Boltzmann constant, respectively. This trend was previously observed in water<sup>18–21,29–31,45–49</sup> and in other liquids.<sup>20,21,38–40,50–53</sup> Even though an Arrhenius  $T$ -dependence can nicely interpolate the present experimental data, as well data at higher temperatures,<sup>18–21</sup> we have to remark that recent results obtained by femtosecond optical Kerr effect demonstrate how a  $T$ -range as the one investigated here is probably too limited in order to reliably distinguish between an Arrhenius law and other  $T$ -trends, such as the Speedy–Angell relation.<sup>54</sup> In particular, at temperatures lower than the ones probed in the present work a clear deviation from the Arrhenius trend is observed.<sup>15,16</sup> Indeed, in such a supercooled phase of water the  $T$ -dependence of  $\tau$  can be approximated by functions, such as the Speedy–Angell relation, which properly accounts for the dynamic slowing down of density fluctuations precursor of the liquid-to-glass transition.<sup>13</sup>

By inspecting Fig. 5 one can appreciate that  $E_a$  is clearly not constant with  $\rho$ . In fact, the density change in the slope

FIG. 6.  $\rho$ -dependence of  $E_a$ , the dashed line is Eq. (8).

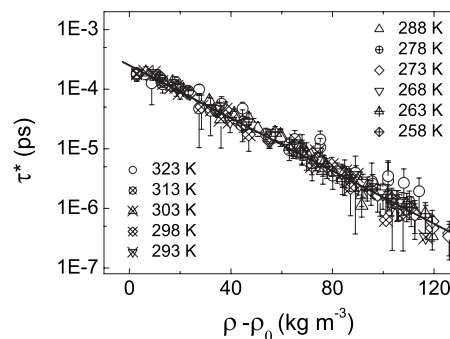
of the straight lines clearly indicates a  $\rho$ -increase in  $E_a$ . Such a  $\rho$ -dependence has not been observed before, most likely because of the lack of a systematic study.

The  $\rho$ -variation of  $E_a$ , as extracted by fitting the constant density data with Eq. (7), is reported in Fig. 6. We found that this trend can be empirically described by a linear law,

$$E_a = E_0 + \alpha(\rho - \rho_0), \quad (8)$$

where  $E_0 = 23.2 \pm 0.5$  kJ mol<sup>-1</sup>,  $\alpha = 1.61 \pm 0.11$  Pa m<sup>6</sup> mol<sup>-2</sup>, and  $\rho_0 = 1000$  kg m<sup>-3</sup>.  $E_0$  therefore represents the activation energy of the relaxation at  $\rho = 1000$  kg m<sup>-3</sup>, while the empirical parameter  $\alpha$  can be regarded as the density coefficient of  $E_a$ , i.e.,  $\alpha = \partial E_a / \partial \rho$ .

We recall that the employed method does not allow to *a priori* associate a specific dynamical process to the relaxation. Consequently,  $E_a$  has to be regarded as an average energy barrier for activating the various processes resulting into a relaxation of density fluctuations. However, we notice that the obtained value for  $E_0$  is on the same order as previous determinations,<sup>18–20,29,45,48,49,54</sup> and similar to the HB potential energy depth.<sup>1,55,56</sup> Moreover, by considering that in these thermodynamic conditions water has an average of 2 HB/molecule,<sup>1,55,56</sup> our determination of  $E_0$  is roughly twice the activation energy associated to HB dynamics, as determined by computer simulations.<sup>46,47</sup> The similarity between  $E_a$  and the HB activation energy was usually invoked to argue that the leading physical process responsible for the relaxation is the continuous rearrangement of HB network through the making/breaking of intermolecular bonds.<sup>18–21,29,30</sup> An analogous parallelism between the intermolecular bond energy and the activation energy of the relaxation of density fluctuation observed in the picosecond time scale was found both in other HB (Refs. 38–40, 50, and 51) and non-HB systems.<sup>21,51–53</sup> Therefore, the obtained result for  $E_0$  further stresses that this relaxation process is essentially related to the collective reorganization of local HB network. Finally, the difference between our finding and a previous experimental determination of  $E_0$  obtained by the analysis of  $S(Q, \omega)$  as measured by IXS (i.e.,  $16 \pm 2.5$  kJ mol<sup>-1</sup>) (Ref. 18) may be ascribed to the complex nature of HB dynamics in water. Indeed, it has been shown that in water the HB energy can assume a continuum range of values due to HB distortions.<sup>57</sup> These strained HBs may relax into the unstrained configuration on the time scale (much less than picosecond) of basic molecular motions (e.g., librations, vibrations, etc.). These motions are faster as

FIG. 7.  $\rho$ -dependence of  $\tau^*$  for all investigated temperatures, the full line is Eq. (9).

compared to the structural relaxation time scales ( $\tau \gtrsim$  ps), and fall definitely out the time window probed by IUVS. Therefore, the relatively slow LA modes detected by IUVS ( $\Omega_L \approx 0.1$  THz) are unlikely affected by these dynamics. On the other hand, IXS probes LA modes with  $\Omega_L$ -values definitely within the 10 THz range and, therefore, can be influenced by fast molecular motions. In IXS experiments these very fast dynamics are empirically accounted for by introducing further relaxation processes,<sup>18–21,32,37–39</sup> but their possible effects on the structural relaxation were not explicitly taken into account. This might affect the proper determination of  $\tau$ .

The  $\rho$ -dependence of  $\tau$  obtained by combining Eqs. (7) and (8) cannot describe the observed decrease in  $\tau$  for increasing  $\rho$  at constant  $T$  (see Fig. 4) since a  $\rho$ -increase in  $E_a$  corresponds to a  $\rho$ -increase in  $\tau$ . Consequently, a further  $\rho$ -dependence has to be introduced in order to fit the experimental data. This can be conveniently derived by introducing the quantity  $\tau^* = \tau / \exp\{E_a / k_B T\}$ . Figure 7 shows  $\tau^*$  as a function of  $\rho$  for all investigated temperatures. All data can be empirically approximated by the following law:

$$\tau^* = \tau_0 \exp\{-\sigma(\rho - \rho_0)\}, \quad (9)$$

where  $\tau_0 = 0.285 \pm 0.01$  fs and  $\sigma = 51.7 \pm 1.0 \times 10^{-3}$  m<sup>3</sup> kg<sup>-1</sup>.

## V. DISCUSSION

In Sec. IV we reported on the  $(\rho, T)$ -dependence of water structural relaxation time in the thermodynamic region ranging from room pressure up to 4000 bars and from 323 K down to the melting temperature.

We found that the  $T$ -dependence of  $\tau$  essentially follows an Arrhenius trend (Fig. 5), while its  $\rho$ -behavior is driven by two competing effects: (i) the  $\rho$ -increase in  $E_a$  (Fig. 6), which leads to a  $\rho$ -increase in  $\tau$ , and (ii) a monotonic  $T$ -independent exponential  $\rho$ -decrease (Figs. 4 and 7). The resulting  $(\rho, T)$ -dependence is therefore

$$\tau = \tau_0 \exp\left\{\frac{E_0 + (\alpha - T k_B \sigma)(\rho - \rho_0)}{k_B T}\right\}. \quad (10)$$

From a dimensional point of view, the quantity  $k_B \sigma$  appearing in Eq. (10) can be regarded as a density coefficient of an activation entropy ( $S_a$ ), i.e.,  $k_B \sigma = \partial S_a / \partial \rho$ , where  $S_a = S_0 + k_B \sigma(\rho - \rho_0)$ . Since in the probed time scale (approximately

equal to picosecond) the relaxation process is mainly related with the collective rearrangements of the local HB network, it is reasonable to assume that  $S_a$ , in analogy with  $E_a$ , is the entropic contribution associated with these dynamics. The coefficient  $(\alpha - Tk_B\sigma)$  appearing in the exponent of Eq. (10) has therefore the structure of a density coefficient of an activation Helmholtz free energy, ( $A_a = E_a - TS_a$ ), related to the local HB network. We can thus rewrite Eq. (10) as

$$\tau = \tau_1 \exp\left\{\frac{A_0 + (\partial A/\partial\rho)(\rho - \rho_0)}{k_B T}\right\}, \quad (11)$$

where  $\tau_1 = \tau_0 \exp\{-S_0/k_B\}$ ,  $A_0 = E_0 - TS_0$ , and  $\partial A/\partial\rho = (\partial E_a/\partial\rho) - T(\partial S_a/\partial\rho) = \alpha - Tk_B\sigma$ .

Equation (11) tells us that the structural relaxation is not only driven by the activation energy of intramolecular bonds, as usually inferred,<sup>18–21,29,31,48,49</sup> but rather to an activation Helmholtz free energy composed by energy-related ( $E_a$ ) and entropy-related ( $TS_a$ ) terms. Within the accuracy of the present data the  $\rho$ -dependence of  $A_a$  can be modeled as a first-order expansion around  $\rho_0$ , i.e.,  $A_a(\rho) = A_0 + (\partial A_a/\partial\rho)(\rho - \rho_0)$ , while no explicit  $T$ -dependence is observed. This  $T$ -dependence, if any, falls beyond the accuracy of the present data. Following this line of thought, the observed decrease in  $\tau$  with increasing  $\rho$  simply reflects the  $\rho$ -increase in  $S_a$ . This implies that more entropic and, therefore, more favorable local equilibrium thermodynamic states are accessible at high density and, consequently, it is easier for the system to relax toward them. This behavior is somehow expected in liquid water at low temperature, where a  $\rho$ -increase in total entropy ( $S$ ) is observed.<sup>41</sup> However, the  $\rho$ -trend of  $S_a$  does not merely parallel the one of  $S$  since the latter increases with  $\rho$  only at  $T \lesssim 5^\circ\text{C}$  at the lower densities.<sup>41</sup> This qualitative comparison suggests that  $S_a$  could significantly contribute to  $S$  at low  $T$ 's and  $\rho$ 's.

We now recall that the leading idea at the base of the liquid-liquid phase transition hypothesis is that normal liquid water at low (high) density behaves more as LDL (HDL), and this “frustrated” situation is responsible for the observed anomalies. Moreover, since the LDA structure is similar to that of crystalline ice while HDA exhibits a higher degree of structural disorder,<sup>58,59</sup> the LDL-HDL phase transition takes place because of the entropy gain associated with the disruption of the relatively ordered, LDA-like, local structures with the consequent formation of HDA-like structures. This picture was first formalized by Poole *et al.*<sup>4</sup> that also proposed a simple model (afterward revised by Jeffery and Austin<sup>56</sup>) able to describe the thermodynamic peculiarities of water.<sup>55,56</sup> These models are based on a van der Waals<sup>55</sup> (or a Song, Mean and Ihm) (Refs. 56 and 60) equation of state modified in order to include the HB contribution. The latter was treated in a mixture model frame, where molecules having open tetrahedral HBs are classified as a different species of water able to generate its own pressure.<sup>61–63</sup> These HBs are similar to the ones occurring in crystalline ice  $I_h$ , in the LDA, and presumably, in the LDL phase. The molar entropy of formation ( $S_{HB}$ ) of such tetrahedral HBs was estimated to be  $\approx 90$  or  $\geq 50$  J mol<sup>-1</sup> K<sup>-1</sup>.<sup>55,56</sup> Using the empirical density coefficient of activation entropy ( $k_B\sigma$ ) extracted from our data, one can estimate the entropy difference associated

with a density jump similar to that observed in the LDA-HDA phase transition (i.e.,  $\Delta\rho \approx 150$  kg m<sup>-3</sup>).<sup>6,58,59</sup> This results in a value of  $\approx 65$  J mol<sup>-1</sup> K<sup>-1</sup>, which is on the same order as  $S_{HB}$ . Although the application of the parameter  $k_B\sigma$  (extracted from data on normal liquid water) to a solid-solid phase transition taking place at much lower temperature is rather unseemly, the similarity between  $S_{HB}$  and  $k_B\sigma\Delta\rho$  stresses how our data are compatible with the picture that attributes the stability of the high-density, HDA-like, water structures to an entropy gain associated with the disruption of such “strong” tetrahedral HBs. On a dynamical point of view, such an entropy gain at high-density can explain the observed  $\rho$ -decrease in  $\tau$  in normal liquid water, and the consequent enhanced fluidity.<sup>44</sup> However, while shear viscosity ( $\eta_s$ ) increases again above  $\rho \approx 1030$ – $1050$  kg/m<sup>3</sup>,  $\tau$  monotonically decreases (see Fig. 4). This behavior is somehow unexpected since it is usually inferred that  $\eta_s \propto \tau$ . Nevertheless, this assumption is based on the underlying hypothesis that the relaxation processes affecting the shear and compressional responses of the fluid are the same. In the present case the relaxation time was extracted from the dispersion of longitudinal sound velocity, which is related to the compressional response of the fluid. The different  $\rho$ -trends of  $\eta_s$  and  $\tau$  could then be ascribed to a different  $\rho$ -dependence of shear and compressional viscosity, a peculiarity already observed in water through sound absorption measurements.<sup>64</sup> This behavior was attributed to a marked  $\rho$ -decrease in the sound absorption in excess of the shear losses. According to authors' claims this also reflects in a  $\rho$ -decrease in  $\tau$ , which is in qualitative agreement with our findings (see Table IV of Ref. 64). Unfortunately, from the present data we cannot quantitatively investigate on possible differences in the shear and compressional relaxation processes, also in light of the poorness of literature data on the  $(\rho, T)$ -dependence of compressional viscosity. Therefore, although this kind of study is of potentially great interest and surely calls for further investigations, it falls beyond the aim of the present work. Finally, it is possible to estimate the temperature ( $T^* = \alpha/(k_B\sigma) = 209 \pm 15$  K), where the  $\rho$ -dependence of  $A_a$  vanishes. In correspondence of this temperature an arbitrary density change would not affect the value of  $\tau$  since, e.g., the  $\rho$ -increase in  $E_a$  cancels the thermodynamic advantage of accessing more entropic local structures at high density, and vice versa. In other words, the activation Helmholtz free energy of the structural relaxation time (that, as previously stated, is an average measure of the rearrangements of water local structure) does not depend on the amount of icelike structures. We also noticed that  $T^*$  falls in the range of the estimated values for the critical temperature of the LDL-HDL phase transition.<sup>2–4,55,65</sup> On the other hand, the density at which the  $T$ -dependence of  $A_a$  (if any) vanishes cannot be derived since an explicit  $T$ -dependence of  $A$  cannot be extracted within the accuracy of the present experimental data.

## VI. CONCLUSIONS

In conclusions, we collected IUVS spectra of liquid water in a range of thermodynamic parameters (i.e.,  $P = 1$ – $4000$  bars,  $T = T_M - 323$  K), where most of water

anomalies are observed. The analysis of viscoelastic behavior of LA modes allowed determining the density and temperature dependence of structural relaxation time.

In all the investigated thermodynamic range we found a clear Arrhenius  $T$ -dependence of  $\tau$  at constant density, as previously observed both experimentally and by computer simulations. Moreover, we further noticed that the activation energy of such Arrhenius trends linearly increases with  $\rho$ . However, this  $\rho$ -dependence cannot account for the observed monotonic density decrease in  $\tau$  at constant temperature. Another density dependence, modeled as a  $T$ -independent exponential  $\rho$ -decay, was then introduced in order to fit the experimental data.

By exploiting a basic dimensional argument, we ascribed the origin of this exponential  $\rho$ -decay to the activation entropy of the relaxation. Therefore, different from earlier results, we found that the structural relaxation process is not simply driven by a simple activation energy related to collective rearrangements of local HB network, but an entropic term has to be introduced. The combined entropy and energy contributions can be regarded as an activation Helmholtz free energy associated with the local (microscopic) water structure. The  $(\rho, T)$ -behavior of such activation free energy may mirror a continuous change in water local structure with increasing density from low-to high-entropy configurations. Because of the higher entropy, high-density structures present an enhanced thermodynamic stability that, on a dynamic point of view, reflects in lower values of relaxation time. These considerations highlight the consistency of our findings with the anomalous behavior of water itself, thus supporting the correctness of the above experimental results and interpretation.

Finally, by extrapolating the data obtained in normal liquid water at lower temperature we also obtained an agreement with mixture models describing water anomalies in the frame of the liquid-liquid phase transition hypothesis. Indeed, the density dependence of the activation free energy vanishes in correspondence of the estimated critical temperature for the LDL-HDL phase transition. At this temperature the high-density entropy gain is counterbalanced by the increase in activation energy. Therefore, the formation/disruption of ordered water structures does not affect the microscopic dynamics of the system. Finally, the density coefficient of the activation entropy is compatible with the estimated entropy gain associated with the disruption of open, icelike structures across a phase transition characterized by a density change similar to the LDA-HDA one. Although the results reported in this manuscript are compatible with the liquid-liquid phase transition hypothesis, further studies in the supercooled phase would be helpful in order to better assess the connections between the relaxation phenomenology of normal liquid water and the postulated liquid-liquid phase transition.

## ACKNOWLEDGMENTS

We gratefully acknowledge Professor Alfonso Franciosi for critical reading of the manuscript. We are also extremely grateful to Dr. Emanuele Pontecorvo for providing  $c_{\infty}(\rho, T)$  data.

- <sup>1</sup> *Water: A Comprehensive Treatise*, edited by F. Franks (Plenum, New York, 1972).
- <sup>2</sup> O. Mishima and H. E. Stanley, *Nature (London)* **396**, 329 (1998).
- <sup>3</sup> P. G. Debenedetti, *J. Phys.: Condens. Matter* **15**, R1669 (2003).
- <sup>4</sup> P. H. Poole, F. Sciortino, U. Essmann, and H. E. Stanley, *Nature (London)* **360**, 324 (1992).
- <sup>5</sup> S. Sastry, P. G. Debenedetti, F. Sciortino, and H. E. Stanley, *Phys. Rev. E* **53**, 6144 (1996).
- <sup>6</sup> E. L. Gromnitskaya, O. V. Stalgorova, V. V. Brazhkin, and A. G. Lyapin, *Phys. Rev. B* **64**, 094205 (2001).
- <sup>7</sup> J. L. Finney, D. T. Bowron, A. K. Soper, T. Loerting, E. Mayer, and A. Hallbrucker, *Phys. Rev. Lett.* **89**, 205503 (2002).
- <sup>8</sup> T. Loerting, C. Salzmann, I. Kohl, E. Mayer, and A. Hallbrucker, *Phys. Chem. Chem. Phys.* **3**, 5355 (2001).
- <sup>9</sup> N. Giovambattista, H. E. Stanley, and F. Sciortino, *Phys. Rev. E* **72**, 031510 (2005).
- <sup>10</sup> A. K. Soper and M. A. Ricci, *Phys. Rev. Lett.* **84**, 2881 (2000).
- <sup>11</sup> M.-C. Bellissent-Funel and L. Bosio, *J. Chem. Phys.* **102**, 3727 (1995).
- <sup>12</sup> C. A. Tulk, C. J. Benmore, J. Urquidi, D. D. Klug, J. Neuefeind, B. Tomberli, and P. A. Egelstaff, *Science* **297**, 1320 (2002).
- <sup>13</sup> W. Gotze and L. Sjogren, *Rep. Prog. Phys.* **55**, 241 (1992).
- <sup>14</sup> L. P. Rebelo, P. G. Debenedetti, and S. Sastry, *J. Chem. Phys.* **109**, 626 (1998).
- <sup>15</sup> R. Torre, P. Bartolini, and R. Righini, *Nature (London)* **428**, 296 (2004).
- <sup>16</sup> C. Masciovecchio, S. C. Santucci, A. Gessini, S. Di Fonzo, G. Ruocco, and F. Sette, *Phys. Rev. Lett.* **92**, 255507 (2004).
- <sup>17</sup> C. Masciovecchio, F. Bencivenga, and A. Gessini, *Condens. Matter Phys.* **11**, 47 (2008).
- <sup>18</sup> G. Monaco, A. Cunsolo, G. Ruocco, and F. Sette, *Phys. Rev. E* **60**, 5505 (1999).
- <sup>19</sup> F. Bencivenga, A. Cunsolo, M. Krisch, G. Monaco, G. Ruocco, and F. Sette, *Phys. Rev. E* **75**, 051202 (2007).
- <sup>20</sup> F. Bencivenga, A. Cunsolo, M. Krisch, G. Monaco, G. Ruocco, and F. Sette, *J. Chem. Phys.* **130**, 064501 (2009).
- <sup>21</sup> F. Bencivenga, A. Cunsolo, M. Krisch, G. Monaco, L. Orsingher, G. Ruocco, F. Sette, and A. Vispa, *Phys. Rev. Lett.* **98**, 085501 (2007).
- <sup>22</sup> F. Bencivenga, A. Cimattoribus, D. Fiocco, A. Gessini, M. G. Izzo, and C. Masciovecchio, *Philos. Mag.* **88**, 4137 (2008).
- <sup>23</sup> See: <http://www.elettra.trieste.it/experiments/beamlines/iuvs/index.html>.
- <sup>24</sup> S. C. Santucci, D. Fioretto, L. Comez, A. Gessini, and C. Masciovecchio, *Phys. Rev. Lett.* **97**, 225701 (2006).
- <sup>25</sup> J. P. Boon and S. Yip, *Molecular Hydrodynamics* (McGraw-Hill, New York, 1980).
- <sup>26</sup> P. Schiebener, J. Straub, J. M. H. Levelt Sengers, and J. S. Gallagher, *J. Phys. Chem. Ref. Data* **19**, 677 (1990).
- <sup>27</sup> F. Sette, G. Ruocco, M. Krisch, C. Masciovecchio, and R. Verbeni, *Phys. Scr.* **T66**, 48 (1996).
- <sup>28</sup> F. Sette, M. H. Krisch, C. Masciovecchio, G. Ruocco, and G. Monaco, *Science* **280**, 1550 (1998).
- <sup>29</sup> G. Ruocco and F. Sette, *J. Phys.: Condens. Matter* **11**, R259 (1999).
- <sup>30</sup> A. Cunsolo, G. Ruocco, F. Sette, C. Masciovecchio, A. Mermet, G. Monaco, M. Sampoli, and R. Verbeni, *Phys. Rev. Lett.* **82**, 775 (1999).
- <sup>31</sup> A. Cunsolo and M. Nardone, *J. Chem. Phys.* **105**, 3911 (1996).
- <sup>32</sup> E. Pontecorvo, M. Krisch, A. Cunsolo, G. Monaco, A. Mermet, R. Verbeni, F. Sette, and G. Ruocco, *Phys. Rev. E* **71**, 011501 (2005).
- <sup>33</sup> E. Herzfeld and T. A. Litovitz, *Absorption and Dispersion of Ultrasonic Waves* (Academic, New York, 1959).
- <sup>34</sup> C. M. Davis and T. A. Litovitz, in *Physical Acoustics*, edited by W. P. Mason (Academic, New York, 1969).
- <sup>35</sup> J. J. Markham, R. T. Beyer, and R. B. Lindsay, *Rev. Mod. Phys.* **23**, 353 (1951).
- <sup>36</sup> M. Krisch, P. Loubeyre, G. Ruocco, F. Sette, A. Cunsolo, M. D'Astuto, R. LeToullec, M. Lorenzen, A. Mermet, G. Monaco, and R. Verbeni, *Phys. Rev. Lett.* **89**, 125502 (2002).
- <sup>37</sup> T. Scopigno, G. Ruocco, and F. Sette, *Rev. Mod. Phys.* **77**, 881 (2005).
- <sup>38</sup> P. Giura, R. Angelini, F. Datchi, G. Ruocco, and F. Sette, *J. Chem. Phys.* **127**, 084508 (2007).
- <sup>39</sup> R. Angelini, P. Giura, D. Fioretto, G. Monaco, G. Ruocco, and F. Sette, *Phys. Rev. B* **70**, 224302 (2004).
- <sup>40</sup> A. Giugni and A. Cunsolo, *J. Phys.: Condens. Matter* **18**, 889 (2006).
- <sup>41</sup> W. Wagner and A. Pruss, *J. Phys. Chem. Ref. Data* **31**, 387 (2002).
- <sup>42</sup>  $c_{\infty}(\rho, T)$  data obtained from IXS spectra showed in Ref. 32 are from E. Pontecorvo (private communication).
- <sup>43</sup> P. B. Macedo and T. A. Litovitz, *J. Chem. Phys.* **42**, 245 (1965).

- <sup>44</sup> K. E. Bett and J. B. Cappi, *Nature (London)* **207**, 620 (1965).
- <sup>45</sup> W. M. Slie, A. R. Donfor, Jr., and T. A. Litovitz, *J. Chem. Phys.* **44**, 3712 (1966).
- <sup>46</sup> F. W. Starr, J. K. Nielsen, and H. E. Stanley, *Phys. Rev. E* **62**, 579 (2000).
- <sup>47</sup> A. Luzar, *J. Chem. Phys.* **113**, 10663 (2000).
- <sup>48</sup> S.-H. Chen and J. Teixeira, *Adv. Chem. Phys.* **64**, 1 (1986).
- <sup>49</sup> C. J. Montrose, J. A. Bucaro, J. Marshall-Coakley, and T. A. Litovitz, *J. Chem. Phys.* **60**, 5025 (1974).
- <sup>50</sup> D. A. Turton and K. Wynne, *J. Chem. Phys.* **128**, 154516 (2008).
- <sup>51</sup> M. D. Ediger, C. A. Angell, and S. R. Nagel, *J. Phys. Chem.* **100**, 13200 (1996).
- <sup>52</sup> T. Kanaya, K. Kaji, and K. Inoue, *Macromolecules* **24**, 1826 (1991).
- <sup>53</sup> C. A. Angell, *J. Non-Cryst. Solids* **131–133**, 13 (1991).
- <sup>54</sup> K. Winkler, J. Lindner, H. Bürsing, and P. Vöhringer, *J. Chem. Phys.* **113**, 4674 (2000).
- <sup>55</sup> P. H. Poole, F. Sciortino, T. Grande, H. E. Stanley, and C. A. Angell, *Phys. Rev. Lett.* **73**, 1632 (1994).
- <sup>56</sup> C. A. Jeffery and P. H. Austin, *J. Chem. Phys.* **110**, 484 (1999).
- <sup>57</sup> J. D. Smith, C. D. Cappa, K. R. Wilson, R. C. Cohen, P. L. Geisseler, and R. J. Saykally, *Proc. Natl. Acad. Sci. U.S.A.* **102**, 14171 (2005).
- <sup>58</sup> J. L. Finney, A. Hallbrucker, I. Kohl, A. K. Soper, and D. T. Bowron, *Phys. Rev. Lett.* **88**, 225503 (2002).
- <sup>59</sup> I. Okabe, H. Tanaka, and K. Nakanishi, *Phys. Rev. E* **53**, 2638 (1996).
- <sup>60</sup> G. Ihm, Y. Song, and E. Mason, *J. Chem. Phys.* **94**, 3839 (1991).
- <sup>61</sup> M. Vedamuthu, S. Singh, and G. W. Robinson, *J. Phys. Chem.* **98**, 2222 (1994).
- <sup>62</sup> M. Vedamuthu, S. Singh, and G. W. Robinson, *J. Phys. Chem.* **99**, 9263 (1995).
- <sup>63</sup> R. L. Lamanna, M. Delmelle, and S. Cannistraro, *Phys. Rev. E* **49**, 2841 (1994).
- <sup>64</sup> T. A. Litovitz and E. H. Carnevale, *J. Appl. Phys.* **26**, 816 (1955).
- <sup>65</sup> S. S. Borick, P. G. Debenedetti, and S. Sastry, *J. Phys. Chem.* **99**, 3781 (1995).